Published in final edited form as:
J Phys Chem B. 2006 November 30; 110(47): 24171–24180. doi:10.1021/jp064361y.

The Guanine Cation Radical: Investigation of Deprotonation States by ESR and DFT

Amitava Adhikary[a], **Anil Kumar**, **David Becker**, and **Michael D. Sevilla**[*]
Department of Chemistry, Oakland University, Rochester, MI 48309

Abstract

This work reports ESR studies that identify the favored site of deprotonation of the guanine cation radical ($G^{\bullet+}$) in an aqueous medium at 77 K. Using ESR and UV-visible spectroscopy, one-electron oxidized guanine is investigated in frozen aqueous D_2O solutions of 2′-deoxyguanosine (dGuo) at low temperatures at various pHs at which the guanine cation, $G^{\bullet+}$ (pH 3–5), singly deprotonated species, G(-H)• (pH 7–9) and doubly deprotonated species, $G(-2H)^{\bullet-}$ (pH>11) are found. C-8-deuteration of dGuo to give 8-D-dGuo removes the major proton hyperfine coupling at C-8. This isolates the anisotropic nitrogen couplings for each of the three species and aids our analyses. These anisotropic nitrogen couplings were assigned to specific nitrogen sites by use of ^{15}N substituted derivatives at N1, N2 N3 atoms in dGuo. Both ESR and UV-visible spectra are reported for each of the species: $G^{\bullet+}$, G(-H)•, and $G(-2H)^{\bullet-}$. The experimental anisotropic ESR hyperfine couplings are compared to those obtained from DFT calculations for the various tautomers of G(-H)•. Using the B3LYP/6–31G(d) method, the geometries and energies of $G^{\bullet+}$ and its singly deprotonated state in its two tautomeric forms, G(N1-H)• and G(N2-H)•, were investigated. In a non-hydrated state G(N2-H)• is found to be more stable than G(N1-H)• but on hydration with 7 water molecules G(N1-H)• is found to be more stable than G(N2-H)•. The theoretically calculated hyperfine coupling constants (HFCC) of $G^{\bullet+}$, G(N1-H)• and $G(-2H)^{\bullet-}$ match the experimentally observed HFCCs best on hydration with 7 or more waters. For $G(-2H)^{\bullet-}$, the hyperfine coupling constant (HFCC) at the exocyclic nitrogen atom (N2) is especially sensitive to the number of hydrating water molecules; good agreement with experiment is not obtained until 9 or 10 waters of hydration are included.

Keywords

Guanine cation radical; deprotonated guanine cation radical; tautomers; ESR; DFT; Isotopic substitution

Introduction

ESR studies on γ-irradiated DNA or DNA-model structures[1, 2] have shown that at low temperatures cytosine and thymine are the sites of electron gain, whereas guanine is the site of hole localization (electron loss). This result is in agreement with the electron affinities (EA) and the ionization potentials (IP) of the bases[3], as well as gas phase and aqueous solution redox potential data.[4] Both the stabilization of the guanine cation radical ($G^{\bullet+}$) and the rate of subsequent hole transfer from $G^{\bullet+}$ to hole-acceptor sites has been shown to depend on prototropic equilibria (as shown in scheme 1). [1f, 4b, 5]

*Author for correspondence. E-mail: sevilla@oakland.edu, Phone: 001 248 370 2328, Fax: 001 248 370 2321.
[a]On leave from Department of Chemistry, Rajdhani College, University of Delhi, Raja Garden, Delhi – 110 015, India.

Although much work has been performed on the guanine cation radical, the specific site of deprotonation is still an open question.[4a, b, 5–7] Pulse radiolysis studies with both conductometric and optical detection have shown that in aqueous solutions, 2′-deoxyguanosine (dGuo) is a good Brønsted acid, with a pK_a of 3.9.[1, 4 –7] Pulse radiolysis studies also suggest that deprotonation of $G^{\bullet+}$ in dGuo occurs by loss of a proton from N1 to give G(N1-H)• (scheme 1).[5] At high pH, G(N1-H)• further deprotonates to produce $G(-2H)^{\bullet-}$ (scheme 1) with pK_a = 10.8.[5] It has also been shown that for 5′-dGMP, the presence of the phosphate group does not affect this prototropic equilibria significantly.[4b] We note that the pK_a of the 1-methylguanosine cationic radical (1-Me-Guo$^{\bullet+}$) is 4.7[5], which suggests that, in dGuo, deprotonation from the exocyclic nitrogen (N2) is competitive with deprotonation from N1 (scheme 1). Theoretical calculations support this and show that the energies involved in producing the N1 deprotonated $G^{\bullet+}$, i.e., G(N1-H)•), or the N2 deprotonated $G^{\bullet+}$, i.e., G(N2-H)•, are very similar.[6] It has been proposed that G(N1-H)• would be favored over G(N2-H)• in environments with high dielectric constants, such as water.[6e]

ENDOR studies carried out using X-ray-irradiated single crystals of Guo, dGuo, 5′-dGMP and 3′,5′-cyclic guanosine monophosphate show that G(N2-H)• rather than G(N1-H)• is formed via deprotonation of $G^{\bullet+}$.[7a–d,f,g,i,j,l] An earlier ENDOR study on X-ray-irradiated single crystals of 5′-dGMP that suggested G(N1-H)• was formed[7e] has been questioned. [7b,] An ESR study in aqueous solution and the associated theoretical calculations[7k] suggested that in $G^{\bullet+}$, the site of deprotonation is likely at N1; however, there are no definitive experimental results which show this.

In our laboratory, $G^{\bullet+}$ is produced by one-electron oxidation of dGuo and analogs by $Cl_2^{\bullet-}$ in an aqueous glass (7.5 *M* LiCl in D_2O).[8] Deuteration at C-8 in dGuo reduces the ca. 8 G anisotropic proton hyperfine coupling to a 1.2 G deuteron coupling and thereby narrows the line-widths and improves resolution.[8b,9] Also, we have employed dGuo derivatives having ^{15}N substitution at N2 in dGuo (**[2-^{15}N]-dGuo**), at N1 and at N2 in dGuo (**[1,2-^{15}N]-dGuo**) and at N1, N2 and N3 in dGuo (**[1,2,3-^{15}N]-dGuo**) to verify both the values of the anisotropic N-couplings and the specific sites of those couplings in one electron oxidize dGuo at various pHs. D_2O solutions are employed throughout the ESR experiments as they reduce linewidths and improve resolution, relative to H_2O, by reducing the magnitude of hydrogen couplings for exchangeable hydrogen atoms. Using ESR spectroscopy and theoretical calculations including water molecules as the hydration shell, we are able to identify the preferred site of deprotonation in $G^{\bullet+}$ in this aqueous system. To the best of our knowledge, our analyses of the ESR spectrum of di-deprotonated $G^{\bullet+}$ [i.e., $G(-2H)^{\bullet-}$, scheme 1] is the first in the literature.

Materials and Methods

Compounds used

2′-deoxyguanosine (dGuo) and Lithium Chloride (99% anhydrous, SigmaUltra) were obtained from Sigma Chemical Company (St Louis, MO). Potassium persulfate (crystal) was purchased from Mallinckrodt, Inc. (Paris, KY). We have carried out deuteration at C-8 in the guanine moiety of dGuo according to Huang *et al.*[8b,–10] using triethylamine (TEA) from Fischer Scientific, NJ. The degree of deuteration (≥ 96%) was determined by 1D NMR signal integration employing a Bruker 200 MHz NMR.[8b] **[2-^{15}N]-dGuo, [1,2-^{15}N]-dGuo and [1,2,3-^{15}N]-dGuo** were gifts from Prof. Roger Jones (Rutgers University, NJ).

Sample preparation

About 3 mg of dGu, its ^{15}N substituted derivatives or 8-D-dGuo was dissolved in 1 mL of 7.5 *M* LiCl in D_2O in the presence of 5 mg $K_2S_2O_8$ for preparation of the glassy samples. If

required, the pH was adjusted under ice-cooled conditions by adding the appropriate μL amounts of 1 *M* NaOH in D_2O or concentrated HCl followed by mixing and the samples were prepared quickly.[8b] pH papers were used for measurements of pH. Note "pH" is determined for D_2O solutions. Because of this and because of the high ionic strength of the glasses, the pH values reported here are approximations.[8b] The solutions were then thoroughly bubbled with nitrogen. Using these solutions, the glassy samples were then prepared by cooling to 77 K as reported earlier.[8] All samples are stored at 77 K.[8]

γ-Irradiation

As in our earlier works[8], the glassy samples of dGuo, **its ^{15}N substituted derivatives** and 8-D-dGuo were γ-irradiated with an absorbed dose of 2.5 kGy at 77 K and were also stored at 77 K.

Annealing of samples

As in our earlier work[8] a variable temperature assembly was employed which passed cooled dry nitrogen gas over the sample. A copper-constantan thermocouple was used to monitor temperatures. The glassy samples (7.5 *M* LiCl) were annealed to 150 – 155 K for 10 – 15 min, resulting in loss of (light yellow) $Cl_2^{\bullet -}$ and the concomitant formation of one-electron oxidized dGuo radicals as evidenced by their ESR spectra and color development in the samples: red-violet at pH ≤ 9, and blue at pH ≥ 11.[8b]

Electron Spin Resonance

ESR spectra were taken on a Varian Century Series ESR spectrometer operating at 9.2 GHz with an E-4531 dual cavity, 9-inch magnet and with a 200 mW klystron. After γ-irradiation at 77 K and annealing to 150–155 K, samples were immediately immersed in liquid nitrogen, and an ESR spectrum was recorded at 77 K and 40 dB (20 μW).[8] Fremy's salt (with g = 2.0056, A_N = 13.09 G) was used for field=calibration similar to our previous works.[8] We have carried out the spectral simulations using SimFonia and WIN-EPR (Bruker). As in our previous work with glassy samples[8], a small singlet "spike" from irradiated quartz at g = 2.0006 was subtracted from spectra before analysis.

Simulations of ESR spectra

Simulations of anisotropic ESR spectra were performed with the WIN-EPR (Bruker) program. Anisotropic nitrogen couplings and g values were found by fits of simulated spectra to the 8-D-dGuo experimental spectra of $G^{\bullet +}$, G(-H)•, and $G(-2H)^{\bullet -}$ found as the pH was adjusted to 3, 9 and 12, respectively. These values were then employed in the simulations of the dGuo spectra of these three one electron oxidized species. The major axis of the nitrogen coupling (A_{zz}) was assumed to be colinear with that of the intermediate value of the C8(H) coupling which has near zero anisotropic contribution. This assumes the p_z-orbitals of the π–electron system are coaxial. The radicals in the three prototropic forms were calculated by DFT to be only slightly nonplanar, thus the assumption that A_{zz} for the guanine moiety nitrogen atoms is colinear with A_{zz} for C8(H) is a good approximation. We performed dozens of computer simulations of the ESR spectra for each species and have been able to ascertain error limits of our fits of ±1 G for the largest of the nitrogen anisotropic couplings and ±1 G for each of the three components of the C8(H) anisotropic coupling (see supplemental Figure S1 for examples of simulations which support this.) The smallest nitrogen anisotropic couplings (A_{xx} and A_{yy}) could not be observed as they are small and unresolved (Table 1). They were assumed to be zero in our simulations and the linewidth was adjusted to account for unresolved couplings. With the aid of the same linewidths, the same C8(H) couplings, and the same g values, the anisotropic N hyperfine couplings in $G^{\bullet +}$, G(-H)•, and $G(-2H)^{\bullet -}$ were then further verified by employing ^{15}N (spin = ½, gyromagentic ratio =1.404 with respect to ^{14}N (spin=1)) substituted

derivatives of dGuo - **[2-^{15}N]-dGuo, [1,2-^{15}N]-dGuo and [1,2,3-^{15}N]-dGuo.** Since ^{15}N couplings are 1.404 times those of ^{14}N and have a spin of ½ vs a spin of 1, a substantial change in the resultant spectrum is observed. This provides an excellent test for our analyses based on ^{14}N couplings.

DFT Calculations

Geometries of G•$^{+}$, G(-H)• (singly deprotonated G•$^{+}$ in dGuo) in two different tautomeric forms, and G(-2H)•$^{-}$ (doubly deprotonated G•$^{+}$), including seven and more water molecules were optimized using Becke's three-parameter exchange functionals (B3)[11] with Lee, Yang and Parr's correlational functional (LYP)[12] and 6–31G(d) basis set as implemented in Gaussian03 suite of programs.[13a] It has been noted that to obtain reliable values of isotropic HFCCs, calculations need well-defined basis set.[13b,c] It has been found that reliable values of anisotropic HFCCs can be obtained with the 6–31G(d) basis set employed in this work for hydrated G•$^{+}$, G(-H)• and G(-2H)•$^{-}$. Frequency animation analysis and molecular modeling were done using the JMOL molecular modeling program.[14] Calculated relative stabilities and hyperfine coupling constants (HFCCs) of selected atoms are presented in Tables 2 and 3 (and also in supplement) respectively. The polarized continuum model (PCM) as implemented in Gaussian 03 suite (IEFPCM) based on the Integral Equation Formalism (IEF) model[13] was used to consider the effect of bulk water on the relative stabilities of the two tautomers of G(-H)•.

Results and Discussion

UV-VIS spectra

The UV-visible spectra of the one-electron oxidized dGuo, at different pHs, taken at 77 K in a 7.5 *M* LiCl glass, are shown in Figure 1. These spectra are similar to those reported in the literature for one-electron oxidized Guo and dGuo, in aqueous solution at room temperature.[4a,b, 5] The similarities of UV-Vis spectra for G•$^{+}$ and G(-H)• clearly suggests that these species have a similar electronic nature.

ESR studies

From previous ESR, ENDOR and theoretical studies[6, 7] on G•$^{+}$ in dGuo we expect three major anisotropic couplings, two nitrogen couplings (at N2 and N3) and one hydrogen (at C8 in the guanine moiety). These studies show the spin density at N1 is quite small. Owing to the fact that we use a D_2O solution in our work, the N-H proton couplings at N1 and at N2 are not observable because they are exchangeable and deuterons have smaller magnetic moment than protons. A deuteron shows couplings that are only 15% (1/6.514) that of protons in the same environment.[8b, 9] Therefore, to simplify the spectra, we have also deuterated the C-8 position in dGuo to get 8-D-dGuo and reduce the anisotropic ca. 8 G proton hyperfine coupling to an unresolved deuteron coupling (ca. 1.2 G). This narrows the line-widths and improves resolution significantly.[8b, 9] As a result, we have used 8-D-dGuo at different pHs in 7.5 *M* LiCl glass, to facilitate the analysis for the nitrogen hyperfine couplings and g values. These couplings and g values are then used in the analysis of the corresponding ESR spectra in identically prepared glassy samples of dGuo studied at each pH. Further, employing identically prepared glassy samples of ^{15}N substituted derivatives of dGuo - **[2-^{15}N]-dGuo, [1,2-^{15}N]-dGuo and [1,2,3-^{15}N]-dGuo,** we have verified the assignment to site as well as the magnitude of the ^{14}N couplings in G•$^{+}$, G(-H)•, and G(-2H)•$^{-}$.

Figure 2 shows the effect of pH on the formation of G•$^{+}$ in glassy samples of 8-D-dGuo (Figures 2A – 2C), and of dGuo (Figures 2D – 2F) prepared in 7.5 *M* LiCl glass in D_2O. Figure 3 shows identically prepared samples of [2-^{15}N]-dGuo and of [1,2-^{15}N]-dGuo (Figures 3A – 3C), and of [1,2,3-^{15}N]-dGuo (Figures 3D – 3F).

G•$^{+}$ in 8-D-dGuo, dGuo and in ^{15}N substituted derivatives of dGuo—In Figures 2A and 2D, we show the ESR spectra (black color) of G•$^{+}$ formed in glassy samples of 8-D-dGuo and of dGuo at pH 3 in 7.5 *M* LiCl, after reaction with Cl_2•$^{-}$ as done in our earlier work.[8] At this pH, G•$^{+}$ is not deprotonated. The experimental spectra found in 8-D-dGuo was simulated using the hyperfine couplings and g-values given in Table 1 ("experimental values"). This simulation matches the corresponding experimental spectrum quite well (Figure 2A). Since the nitrogen couplings and radical g-values do not change when the deuteron at C8 is replaced by a proton, the values were then used for the simulation of the spectrum of dGuo. The C8(H) anisotropic couplings for the dGuo radical were those that resulted in a good fit to the experimental dGuo spectrum (Figure 2D, Table 1).

Simulations of the ^{15}N (spin=1/2) substituted ESR spectra for ([2-^{15}N]-dGuo), ([1,2-^{15}N]-dGuo), and ([1,2,3-^{15}N]-dGuo) (Figure 3) for G•$^{+}$, G(-H)• and G(-2H)$^{-}$• were performed using identical parameters as used for the ^{14}N simulations taking only into account the change in coupling and spin for the ^{15}N site. Thus these simulations have not been optimized to fit and provide an excellent test of our analyses for ^{14}N couplings as well as their site assignments. In each case the simulations closely match the experimental spectra.

In Figures 3A–C, C8-H doublet at the center in G•$^{+}$ spectrum is even more prominent than observed for ^{14}N counterparts. This doublet again collapses to a singlet upon deuteration at C8-H in [2-^{15}N]-dGuo (see supplemental Figure S2). We find that G•$^{+}$ formed in [2-^{15}N]-dGuo and in [1,2-^{15}N]-dGuo show identical ESR spectra (Figure 3A) which shows that N1 does not have a significant hyperfine coupling. The match between ESR spectra of G•$^{+}$ formed in [1,2-^{15}N]-dGuo and in [1,2,3-^{15}N]-dGuo (Figures 3A and 3D) with their corresponding simulations verify our ^{14}N –hyperfine couplings magnitudes and sites (Table 1). Further they clearly show that in G•$^{+}$ the hyperfine couplings of N3 are larger than those of N2 (Table 1).

G(-H)• in 8-D-dGuo, dGuo and in ^{15}N substituted derivatives of dGuo—In Figures 2B and 2E, we present the ESR spectra (black) in glassy samples of 8-D-dGuo and of dGuo at pH ca. 9 in 7.5 *M* LiCl, after reaction with Cl_2•$^{-}$. At this pH G•$^{+}$ has undergone a single deprotonation[8b] at N1 (*vide infra*) to form G(-H)• Resolved line components from anisotropic nitrogen atom couplings are visible in wings of these spectra of G(-H)• (Figures 2B, 2E). As was done for G•$^{+}$, nitrogen hyperfine parameters were found by analysis of the experimental spectra of 8-D-dGuo and these values, along with an anisotropic C8-H proton coupling, were used to fit the dGuo spectrum. The simulated spectra (blue color) using these parameters (Table 1, G(N1-H)•) match the corresponding experimentally obtained spectra of G(-H)• in both 8-D-dGuo and dGuo samples; it should be noted that the single deprotonation of G•$^{+}$ has only a small effect on the C8(H) hyperfine couplings. We also note that both UV-vis spectra (Figure 1), and the ESR spectra (Figure 2) of G•$^{+}$ and G(-H)• are very similar for dGuo as well as 8-D-dGuo samples. The similarities in ESR spectra of G•$^{+}$ and G(-H)• are justified by the fact that the spin densities and the associated hyperfine couplings for these two species are similar (Table 1 and Table 3). It is, however, evident from Table 1 and Figure 4 that the g⊥ values of these two radicals differ enough to distinguish the state of protonation with pH.

Again the experimentally obtained N–hyperfine couplings for G(-H)• (Table 1) were validated by ^{15}N nitrogen hyperfine parameters of G(-H)• formed in [1,2-^{15}N]-dGuo and in [1,2,3-^{15}N]-dGuo (Figures 3B and 3E). These spectra clearly establish that (i) in G(-H)• the hyperfine couplings of N3 are larger than those of N2 and (ii) N1 does not have significant hyperfine coupling in the ESR spectra of G(-H)• (Table 1). As we have seen in the spectra for G•$^{+}$ (Figures 2G, 2H), the C8-H doublet at the center also becomes prominent due to ^{15}N isotopic substitution in the spectra of G(-H)• (Figures 3B, 3E and the supplemental Figure S2).

G(-2H)•$^{-}$ in 8-D-dGuo, dGuo and in ^{15}N substituted derivatives of dGuo—From previous work[4a,b, 5], it appears that at pH =12, G•$^{+}$ is doubly deprotonated (at N1 and N2), resulting in **G(-2H)•$^{-}$**. In Figures 2C and 2F, the ESR spectra (black color) of G(-2H)•$^{-}$ formed in glassy samples of 8-D-dGuo and of dGuo at pH ca. 12 in 7.5 *M* LiCl, after reaction with Cl_2•$^{-}$ are shown. Nitrogen hyperfine couplings are nicely resolved in the wings of both spectra. Figure 2C for 8-D-dGuo and Figure 2F for dGuo clearly demonstrate excellent resolution in the wings of the anisotropic N-couplings for **G(-2H)•$^{-}$** for both C8-deuterated and protonated systems. The poorly resolved ca. 5.5 G doublet from C8(H) is lost in 8-D-dGuo as expected. Again, the simulated spectra (green) using the parameters in Table 1 match the experimental spectra well.

ESR spectra of **G(-2H)•$^{-}$ in** [2-^{15}N]-dGuo, [1,2-^{15}N]-dGuo, and [1,2,3-^{15}N]-dGuo are shown in Figures 3C and 3F. Analyses of spectra in shown in the Figures 3C and 3F clearly establish that (i) in the ESR spectrum of of **G(-2H)•$^{-}$**, N1 a significant hyperfine coupling (Table 1) and (ii) unlike the cases of G•$^{+}$ and G(-H)•, N2 has a larger nitrogen hyperfine coupling than N3. The Figure S2 in supporting information shows the collapse of the C8-H doublet on deuteration in [2-^{15}N]-dGuo at various pHs.

From the analyses of the ESR spectra of one-electron-oxidized guanine in 8-D-dGuo and **^{15}N substituted derivatives of dGuo (**[2-^{15}N]-dGuo, [1,2-^{15}N]-dGuo, and [1,2,3-^{15}N]-dGuo**)** at different pHs, we are confident that the anisotropic N-couplings are well determined (±1 G) (see supplemental Figure S3). We note that the increase of the total width in the spectrum on going from 8-D-dGuo to dGuo in each pH range gives the A_{zz}(C8-H) coupling (after properly accounting for the small deuterium coupling). Because the nitrogen couplings are well determined, the C8(H) couplings are likely to also be accurate to within ±1G. Numerous fits which varied the couplings suggest these uncertainties are reasonable (see supplemental Figures S1 and S3). The values of the hyperfine coupling constants for the N2, N3 and C8(H) are in good agreement with the both existing ESR and ENDOR studies[7,8] and with our theoretical calculations (*vide infra*).

The ESR measurements at the various pHs used indicate that the pK_a of G•$^{+}$ in our system (aqueous D_2O glasses at 77 K) is between 5 and 6; this is approximately 1 to 2 pH units higher than the corresponding pK_a (ca. 3.9) of G•$^{+}$ in aqueous H_2O solution 298 K.[1, 4 – 7] This is reasonable considering the system is a D_2O solution (glassy) at low temperature and that pK_as in D_2O are generally higher than the corresponding pK_a's in H_2O (Figure 4).[15] These results are also in accord with our previous work on photo-excitation of G•$^{+}$ in D_2O glass at 77 K, which suggested that G•$^{+}$ does not deprotonate until ca. pH 6.[8]

DFT calculations

Relative stabilities of different tautomeric forms—The presence of different tautomeric forms of G(-H)• in DNA are of considerable interest and of biological significance.[7] ESR measurements give hyperfine couplings which are sensitive to these tautomeric forms and afford an opportunity to find the dominant tautomer in vacuum and an aqueous environment by using a combination of theory and experiment. In this DFT study, we consider three possible tautomers of G(-H)•: (i) deprotonation at N1 to give G(N1-H)• and (ii) deprotonation at either the *syn* or *anti* sites of the NH_2 group with respect to the N3 atom (scheme 1). The geometries of all three tautomers in the presence of a single water molecule, placed near the N1 and NH_2 sites of the molecule, were fully optimized using the B3LYP/6-31G(d) level of theory. The relative stabilities of the three structures G(N1-H)• + H_2O, G(N2-H)•$_{syn}$+H_2O and G(N2-H)•$_{anti}$+H_2O were 2.65, 0.00 and 3.63 kcal/mol, respectively (Table 2). Recently, Schaefer and his co-workers, using the B3LYP/DZP++ level of theory, found that G(N2-H)• was more stable than G(N1-H)• by 4.96 kcal/mol.[6d] To take into account the effect of the solvent better, we performed a single point calculation of the optimized

tautomers G(N1-H)•+H_2O and G(N2-H)•+H_2O in an aqueous environment (ε_0 = 78.4) using the polarized continuum model (IEFPCM) at the B3LYP/6-31G(d) level of theory. Using IEFPCM to model the aqueous environment, G(N2-H)• + H_2O is only 0.90 kcal/mol more stable than G(N1-H)• + H_2O (Table 2).

Regarding the relative stabilities of G(N1-H)• and G(N2-H)•$_{syn}$, in guanine calculated at various theoretical levels are also shown in Table 2. Using different methods and basis sets, Mundy et al.[6b] calculated the relative stabilities of several radicals that were generated from the deprotonation of G•$^+$ at different sites. Their calculations (B3LYP/6-31++G(3df,3pd) // B3LYP/6-31++G(3df,3pd)) showed that G(N2-H)•$_{syn}$ was more stable than G(N1-H)• in the gas phase by 4.71 kcal/mol (see Table 2). However, using the same basis set and the COSMO solvation model to simulate an aqueous environment, they found that G(N1-H)• was more stable than G(N2-H)• by 0.91 kcal/mol. The same trend is found in all reported calculations which agree that G(N2-H)•$_{syn}$ state is more stable than G(N1-H)• in the gas phase by 2.7 to 4.7 kcal/mol[7].

Based on these studies, we have further included the water molecules surrounding the guanine base to test the effects of hydration on the relative stabilities of G(N1-H)• and G(N2-H)•$_{syn}$ (Figure 5). We have fully optimized each structure using B3LYP/6-31G(d) level of calculation including seven water molecules around the guanine base moiety.

These calculations indicate that G(N1-H)• +7 H_2O is more stable than G(N2-H)•$_{syn}$ +7 H_2O by 3.26 kcal/mol (see Table 2). To take into account the effect of full solvent, we have further performed single point calculations using the optimized geometries of G(N1-H)• +7 H_2O and G(N2-H)•$_{syn}$ +7 H_2O along with the IEFPCM model at the B3LYP/6-31G(d) level. These calculations show that G(N1-H)• +7 H_2O is still more stable than G(N2-H)• +7 H_2O by 3.00 kcal/mol (Table 2). Thus our results suggest that hydration is most important on the relative stabilities of these two tautomers.

Hydrogen bond energies—The hydrogen bonding energy arising from seven waters is calculated using the following equation (1):

$$E^{H-bond} = TE^{G(-H)\bullet + 7\,H_2O} - (TE^{G(-H)\bullet} + 7TE^{H_2O}) \quad (1)$$

Here $E^{H\text{-}bond}$ is the hydrogen bond energy. TE is the total energy of optimized (G(-H)• +7 H_2O) complex and $TE^{G(-H)\bullet}$ refers to the total energy of either G(N1-H)• or G(N2-H)•$_{syn}$ tautomer. TE^{H_2O} is the total energy of a single H_2O molecule.

Using equation (1), $E^{H\text{-}bond}$[G(N1-H)•] = −104.1 kcal/mol and, $E^{H\text{-}bond}$[G(N2-H)•$_{syn}$] = −95.6 kcal/mol (Figure 5). Thus, the hydrogen bonding due to hydration stabilizes G(N1-H)• by 8.5 kcal/mol more than it does G(N2-H)•. Note from Figure 5 that the same number of hydrogen bonds (twelve) are present in each system and it is the increased *strength* of the hydrogen bonds in the G(N1-H)• +7 H_2O system that accounts for the additional stabilization energy.

Hyperfine Coupling Constants in G•$^+$ and G(-H)•—On comparing experimental HFCCs with those calculated at various hydration levels (see supplement), we find those calculations using 7 water molecules for G•$^+$, G(N1-H)• and G(N2-H)•$_{syn}$ (Figure 5) and 8–10 water molecules for G(-2H)•$^-$ (Figure 5) in dGuo gave the best fit to experiment (see Table 1 and Table 3).

For G•$^+$+7H_2O, B3LYP/6-31G(d) level of theory predicts two observable A_{zz} nitrogen couplings of 11.8 G for N3, and 9.1 G for N2 and a substantial anisotropic hydrogen coupling for C8(H) of (−7.8, −10.4, −2.4) G. These values are all in good agreement with our

experimental couplings (Table 1). The calculated hyperfine coupling constants for N1 and N7 (Tables 1 and 3) are small and these couplings were not observed in our ESR experiments for $G•^{+}$.

For G(N1-H)• $+7H_2O$, the calculated A_{zz} values for N3 (13.5 G) and N2 (9.1 G), and the calculated anisotropic C8(H) coupling (−8.4, −11.3, −3.0) G, agree well with the corresponding experimental values of 12.0 G, 8.0 G and (−7.2, −10.5, −3.5) G (Table 1). Calculations also indicate that N1 and N7 both have very small couplings (Table 3), in strong agreement with the fact that these couplings were not observed in our ESR experiments. In addition, our calculated anisotropic HFCC for C8(H) is in good agreement with that calculated by Wetmore et al[6a], (−7.0, −11.5, −3.9) G using DFT (P86) with a 6-311G(2d,p) basis set. On the other hand, for G(N2-H)$•_{syn}$+7 H_2O, the calculated A_{zz} HFCCs for N3 (17.6 G) and N2 (15.0 G) and the calculated anisotropic C8(H) coupling (−6.6, −8.8, −2.3) G, do not agree well with the corresponding experimental values. The large calculated A_{zz} for N3 (17.60 G) calculated for G(N2–H)• is not in agreement with the smaller experimental value of 8.0 G. Experiment is in far better agreement with the 9.1G for the N3 A_{zz} coupling predicted for G(N1-H)•. The C8 (H) anisotropic couplings calculated by Wetmore et al[6a] for G(N2-H)• of (-6.3, −9.4, −2.3) G are in close agreement with our calculated values. For G(N2-H)• also, calculations indicate that N1 and N7 have very small couplings (Table 3).

These results strongly suggests that G(N1-H)• is the most stable tautomer present in an aqueous medium and therefore combining the ESR and DFT results, we conclude N1 is the site of deprotonation for $G•^{+}$ in this frozen aqueous glass.

Hyperfine Coupling Constants in G(-2H)•$^{-}$—The calculated A_{zz} for N2 in G(-2H) •$^{-}$depends quite strongly on the number of water molecules included in the model (Figure 6). We found that only on increasing the number of hydration waters to the 9–10 range could we obtain nitrogen A_{zz} couplings that compared favorably with experiment. For G(-2H) •$^{-}$+$9H_2O$, the predicted HFCCs at N3 (14.8, 0.9, 1.0) G, and N2 (17.6, 0.8, 0.8) G and the anisotropic C8(H) coupling (−6.8, −9.3, −2.6) G are in reasonable agreement with the observed couplings (Table 1).

From Figure 6, it is evident that in G(-2H)•$^{-}$, the HFCC (A_{zz}) at N2 atom decreases with increasing number of hydrating water molecules while that of N3 increases. With 10 water molecules these values become nearly equal. We find that the Mulliken spin densities at N2 and N3 atoms are also nearly equal, 0.35 and 0.32. Since G(-2H)•$^{-}$ is negatively charged, and is in solution of 7.5 *M* LiCl (Figure 2), we also performed calculations including Li^{+} as a counter-ion. We find that in the presence 7–10 water molecules, Li^{+} has a very small effect on HFCCs suggesting water hydrogen bonding dominates or the electrostatic effects. However, in the presence of a small number of water molecules Li^{+} effect is substantial with the same effect as for increased hydration (see supplement). Analyses of the ESR spectra (Spectra C, F, Figure 3) for ^{15}N (spin = ½) HFCCs clearly show that for G(-2H)•$^{-}$, N2 site has a slightly larger coupling than N3 in agreement with results shown in Figure 6 at about nine water molecules of hydration.

ESR studies employing 8-D-dGuo at different pH and the complementary theoretical calculations for G(-2H)•$^{-}$ suggest that N7 has only a small isotropic hyperfine coupling (ca. 0.5 G) (Table 3). An earlier computational and ESR study on $G•^{+}$ in aqueous solution suggested a 3 G isotropic coupling at N7[7k] which is significantly larger than we would expect from our work.

Activation Energy of Proton Transfer—To estimate the energetics of water assisted proton transfer between tautomers G(N1-H)• and G(N2-H)•, we have calculated the forward

barrier for the proton transfer between G(N1-H)• $+H_2O$ and G(N2-H)• $+H_2O$ in the presence of a single water molecule (Figure 7). The B3LYP/6-31G(d) level of theory predicts a forward barrier of 18.8 kcal/mol (Figure 7). A frequency calculation shows that the transition state has a single negative frequency -1688 cm^{-1} confirming this is a true transition state which connects the reactant and product. In another recent calculation[6f] using the B3LYP/6-31G* method, and a model in which the sugar moiety was replaced by a methyl group (9-methylguanine), a forward barrier of 18.8 kJ/mol (4.5 kcal/mol) was reported. In our calculation, we considered the full sugar moiety (Figure 7). We therefore repeated their calculation on the 9-methylguanine system and obtained 18.9 kcal/mol for the barrier height (Table 2) suggesting the units may have been incorrectly reported in the previous work. Without any water, the direct proton transfer from N2 to N1 converting G(N1-H)• to G(N2-H)• has been reported to have a much larger barrier of 43.9 kcal/mol.[6f] We note the role of water molecules in promoting proton transfer reactions at much lower activation barriers is expected and has been reported in the literature for HF and MP2 level calculations.[16] Based on the above argument, the presence of a full aqueous medium (where the N1-H tautomer is favored) is expected to reduce the activation barrier significantly (Table 2). The calculation to locate the transition state in the presence of a full hydration shell awaits future efforts as this will require substantial computational time.

Summary and Conclusions

(i) Protropic forms and site of deprotonation in G•+

Our results identify three prototropic forms of one electron oxidized guanine, G•+, G(-H)•, G(-2H)•−, via ESR and UV-vis spectroscopy which are found in the pH ranges 3 –5, 7–9 and >11, respectively.

The experimentally obtained HFCCs for G•+ as well as G(N1-H)• in dGuo match the theoretical values well. Thus, ESR spectroscopy, UV-visible spectroscopy and complimentary theoretical calculations give strong evidence that the N1-H site is the first deprotonation site of G•+ in frozen aqueous (D_2O) glassy solutions.

(ii) Relative stabilities of G(N1-H)• and G(N2-H)• and the role of hydration

Earlier theoretical calculations indicate that G(N2–H)• is more stable than G(N1-H)• in the gas phase by ca. 4.5 kcal/mol. Our work shows that with one additional water molecule, this is reduced to 2.65 kcal/mol. However, with seven waters, the order of stabilization is reversed and G(N1-H)• becomes more stable than G(N2-H)• by ca. 3.3 kcal/mol (Table 2) as a result of the stabilizing effect of H-bonding interactions in the first hydration shell. Surprisingly, employing the IEFPCM solvation model in addition to the 7 waters has little effect on the relative energies of the two tautomers. This finding suggests that the first seven waters are most important in determining the relative stability of the two tautomers. While no experimental value for the difference in energy between the two tautomers is available, our ESR and vis-UV experiments strongly suggest that G(N1-H)• dominates in the aqueous phase, in agreement with theory.

(iii) Transition state for water assisted proton transfer between G(N2-H)• and G(N1-H)•

Using one water molecule, we find a clear transition state for water assisted proton transfer between G(N2-H)• and G(N1-H)•. Our DFT calculations suggest the activation barrier for this transfer is 18.8 kcal/mol. However, under full solvation this value is likely to be significantly lower.

(iv) (G(-2H)•⁻)

The ESR spectrum of **G(-2H)•⁻** was first reported in our earlier work[8b] and, in this work, has been interpreted for the first time. ESR spectra display excellent resolution of two anisotropic N splittings for all the dGuo samples at pH 12 (Figure 2). For G(-2H)•⁻ theoretical calculations suggest a strong dependence of the spin density distribution and hyperfine couplings with the level of hydration. Very poor agreement of experimental couplings with theory occurs for isolated molecules, but agreement is much improved as 9 or 10 water molecules are added.

(v) ^{15}N substituted derivatives of dGuo

The use of ^{15}N substituted derivatives of dGuo verified both the magnitude and site assignment of the nitrogen hyperfine couplings reported for N3, N2 in one-electron oxidized radicals of dGuo in three states of protonation. These results have also shown that: (a) N3 is largest coupling in the one-electron-oxidized guanine radicals for G•⁺ and G(-H)•. (b) For G(-2H)⁻•, N2 is the largest coupling site. (c) N1 has no significant coupling in G•⁺, G(-H)• or G(-2H)•⁻.

Supplementary Material

Refer to Web version on PubMed Central for supplementary material.

Acknowledgements

This work was supported by the NIH NCI under grant no. R01CA045424. The authors are very grateful to Prof. Roger Jones for his very kind donation of the ^{15}N isotopically substituted dGuo derivatives employed in this study. A.A. is grateful to the authorities of the Rajdhani College and the University of Delhi for leave to work on this research program. A.K. and M.D.S. are thankful to Arctic Region Supercomputing center (ARSC) for a generous grant of CPU time and facilities. A.K. is personally thankful to the ARSC staff for their constant cooperation and timely help. We thank D. Khanduri and S. Collins for their aid with the experiments.

References

1. For recent ESR reviews (charge transfer in DNA and in model compounds), see: (a) BeckerDSevillaMDGilbertBCDaviesMJMurphyDMIn Royal Society of Chemistry Specialist Periodical ReportElectron Spin Resonance1998167114 (b) Sevilla MD, Becker D, Gilbert BC, Davies MJ, Murphy DM. Royal Society of Chemistry Specialist Periodical Report. Electron Spin Resonance 2004;19:243–278.(c)CaiZSevillaMDSchusterGBLong Range Charge Transfer in DNA II. Topics In Current ChemistrySpringer-VerlagBerlin, Heidelberg2004237103(d) BernhardWACloseDMMozumdarAHatanoYCharged Particle and Photon Interactions with Matter Chemical, Physicochemical and Biological Consequences with ApplicationsMarcel Dekkar, IncNew York, Basel2004431(e)WagenknechtH-AWagenknechtH-ACharge Transfer in DNA: From Mechanism to ApplicationWilley-VCH Verlag GmbH & CoKGaA, Weiheim20054(f)von SonntagCFree-radical-induced DNA Damage and Its RepairSpringer-VerlagBerlin, Heidelberg2006213
2. (a) Sevilla MD, Becker D, Yan M, Summerfield SR. J Phys Chem 1991;95:3409–3415. (b) Yan M, Becker D, Summerfield SR, Renke P, Sevilla MD. J Phys Chem 1992;96:1983–1989. (c) Wang W, Sevilla MD. Radiat Res 1994:9–17. [PubMed: 8146305] (d) Spaletta RA, Bernhard WA. Radiat Res 1993:143–150. (e) Mrozcka NE, Bernhard WA. Radiat Res 1993;135:155–159. [PubMed: 8396269] (f) Mrozcka NE, Bernhard WA. Radiat Res 1995;144:251–257. [PubMed: 7494867] (g) Cullis PM, Davis AS, Malone ME, Podmore ID, Symons MCR. J Chem Soc Perkin Trans 2;1992:1409–1412. (h) Hüttermann J, Lange M, Ohlmann J. Radiat Res 1992;131:18–23. [PubMed: 1320767] (i) Hüttermann J, Röhrig M, Köhnlein W. Int J Radiat Biol 1992;61:299–313. [PubMed: 1347062]
3. (a) Sovzil D, Jungwirth P, Havlas Z. Collect Czech Chem Commun 2004;69:1395–1428. (b) Kumar A, Knapp-Mohammady M, Mishra PC, Suhai S. J Comput Chem 2004;25:1047–1059. [PubMed: 15067680] (c) Li X, Cai Z, Sevilla MD. J Phys Chem B 2001;105:10115–10123. (d) Li X, Cai Z, Sevilla MD. J Phys Chem A 2002;106:1596–1603. (e) Li X, Cai Z, Sevilla MD. J Phys Chem A

2002;106:9345–9351. (f) Rienstra-Kiracofe JC, Tschumper GS, Schaefer HF III, Nandi S, Ellison GB. Chem Rev 2002;102:231–282. [PubMed: 11782134] (g) Reynisson J, Steenken S. Phys Chem Chem Phys 2002;4:527–532. (h) Close DM. J Phys Chem A 2004;108:10376–10379. (i) Crespo-Hernández CE, Arce R, Ishikawa Y, Gorb L, Leszczynski J, Close DM. J Phys Chem A 2004;108:6373–6377. (j) Close DM, Crespo-Hernández CE, Gorb L, Leszczynski J. J Phys Chem A 2005;109:9279–9283. [PubMed: 16833269] (k) Caruso T, Carutenuto M, Vasca E, Peluso A. J Am Chem Soc 2005;127:15040–15041. [PubMed: 16248639] (l) Wetmore SD, Boyd RJ, Eriksson LA. Chem Phys Lett 2000;322:129–135.

4. (a) Jovanovic SV, Simic MG. J Phys Chem 1986;90:974–978. (b) Jovanovic SV, Simic MG. Biochim Biophys Acta 1989;1008:39–44. [PubMed: 2719961] (c) Seidel CAM, Schulz A, Sauer MHM. J Phys Chem 1996;100:5541–5533. (d) Steenken S, Jovanovic SV. J Am Chem Soc 1997;119:617–618. (e) Baik MH, Silverman JS, Yang IV, Ropp PA, Szalai VS, Thorp HH. J Phys Chem B 2001;105:6437–6444. (f) Langmaier J, Samec Z, Samcova E, Hobza P, Reha D. J Phys Chem B 2004;108:15896–15899. (g) Llano J, Eriksson LA. Phys Chem Chem Phys 2004;6:2426–2433. (h) Fukuzumi S, Miyao H, Ohkubo K, Suenobu T. J Phys Chem A 2005;109:3285–3294. [PubMed: 16833661] (i) Cauet E, Dehareng D, Lievin J. J Phys Chem A 2006;110:00.
5. (a) Candeias LP, Steenken S. J Am Chem Soc 1989;111:1094–1099. (b) Steenken S. Chem Rev 1989;89:503–520. (c) Steenken S. Free Radical Res Commun 1992;16:349–379. [PubMed: 1325399] (d) Steenken S, Jovanovic SV, Candeias LP, Reynisson J. Chem Eur J 2001;7:2829–2833. (e) Kobayashi K, Tagawa S. J Am Chem Soc 2003;125:10213–10218. [PubMed: 12926943]
6. (a) Wetmore SD, Boyd RJ, Eriksson LA. J Phys Chem B 1998;102:9332–9343. (b) Mundy CJ, Colvin ME, Quong AA. J Phys Chem A 2002;106:10063–10071. (c) Gervasio FL, Laio A, Iannuzzi M, Parrinello M. Chem Eur J 2004;10:4846–4852. (d) Luo Q, Li QS, Xie Y, Schaefer HF III. Collect Czech Chem Commun 2005;70:826–836.von Sonntag, C. Free-radical-induced DNA Damage and Its Repair. Springer-Verlag; Berlin, Heidelberg: 2006. p. 220-221. (f) Chatgilialoglu C, Caminal C, Guerra M, Mulazzani QG. Angew Chem Int Ed 2005;44:6030–6032.
7. (a) Close DM, Sagstuen E, Nelson WH. J Chem Phys 1985;82:4386–4388. (b) Hole E, Nelson WH, Close DM, Sagstuen E. J Chem Phys 1987;88:5218–5219. (c) Close DM, Nelson WH, Sagstuen E. Radiat Res 1987;112:283–301. [PubMed: 2825232] (d) Hole EO, Sagstuen E. Radiat Res 1987;109:190–205. [PubMed: 3027741] (e) Ravkin B, Herak JN, Voit K, Hüttermann J. Radiat Environ Biophys 1987;26:1–12. [PubMed: 3035602] (f) Nelson WH, Hole EO, Sagstuen E, Close DM. Int J Radiat Biol 1988;54:963–986. [PubMed: 2903893] (g) Hole EO, Sagstuen E, Nelson WH, Close DM. Free Radical Res Commun 1989;6:87–90. [PubMed: 2545565] (h) Kim H, Budzinski EE, Box HC. J Chem Phys 1989;90:1448–1451. (i) Hole EO, Sagstuen E, Nelson WH, Close DM. Radiat Res 1991;125:119–128. [PubMed: 1847530] (j) Hole EO, Sagstuen E, Nelson WH, Close DM. Radiat Res 1992;129:1–10. [PubMed: 1309400] (k) Bachler V, Hildenbrand K. Radiat Phys Chem 1992;40:59–68. (l) Hole EO, Sagstuen E, Nelson WH, Close DM. Radiat Res 1992;129:119–138. [PubMed: 1310357]
8. (a) Shukla LI, Pazdro R, Huang J, DeVreugd C, Becker D, Sevilla MD. Radiat Res 2004;161:582–590. [PubMed: 15161365] (b) Adhikary A, Malkhasian AYS, Collins S, Koppen J, Becker D, Sevilla MD. Nucleic Acids Res 2005;33:5553–5564. [PubMed: 16204456] (c) Adhikary A, Kumar A, Sevilla MD. Radiat Res 2006;165:479–484. [PubMed: 16579661]
9. Hiraoka W, Kuwabara M, Sato F. Int J Radiat Biol 1989;55:51–58. [PubMed: 2562976]and the references therein
10. Huang X, Yu P, LeProust E, Gao X. Nucleic Acids Res 1997;25:4758–4763. [PubMed: 9365253]
11. (a) Becke AD. J Chem Phys 1993;98:1372. (b) Stephens PJ, Devlin FJ, Frisch MJ, Chabalowski CF. J Phys Chem 1994;98:11623.
12. Lee C, Yang W, Parr RG. Phys Rev B 1988;37:785.
13. Frisch, MJ., et al. Gaussian 03, revision B.04. Gaussian, Inc; Pittsburgh, PA: 2003. Malikn, VG.; Malkina, OL.; Eriksson, LA.; Salahub, D. Modern Density Functional Theory, A Tool for Chemistry. Seminario, JM.; Politzer, P., editors. Elsevier; New York: 1995. (c) Engels B, Eriksson LA, Lunell S. Adv Quantum Chem 1997;27:297. (d) Cancès MT, Mennucci B, Tomasi J. J Chem Phys 1997;107:3032. (e) Mennucci B, Tomasi J. J Chem Phys 1997;106:5151. (f) Mennucci B, Cancès E, Tomasi J. J Phys Chem B 1997;101:10506. (g) Tomasi J, Mennucci B, Cancès E. J Mol Struct (Theochem) 1999;464:211.

14. http://jmol.sourceforge.net

15. (a) Pentz L, Thornton ER. J Am Chem Soc 1967;89:6931–6938.and the references therein (b) Washabaugh MW, Jencks WP. Biochemistry 1988;27:5044–5053. [PubMed: 2844248] (c) Krezel A, Bal W. J Inorg Biochem 2004;98:161–166. [PubMed: 14659645]and the references therein

16. (a) Gorb L, Leszczynski J. J Am Chem Soc 1998;120:5024. (b) Llano J, Eriksson LA. Phys Chem Chem Phys 2004;6:4707–4713.

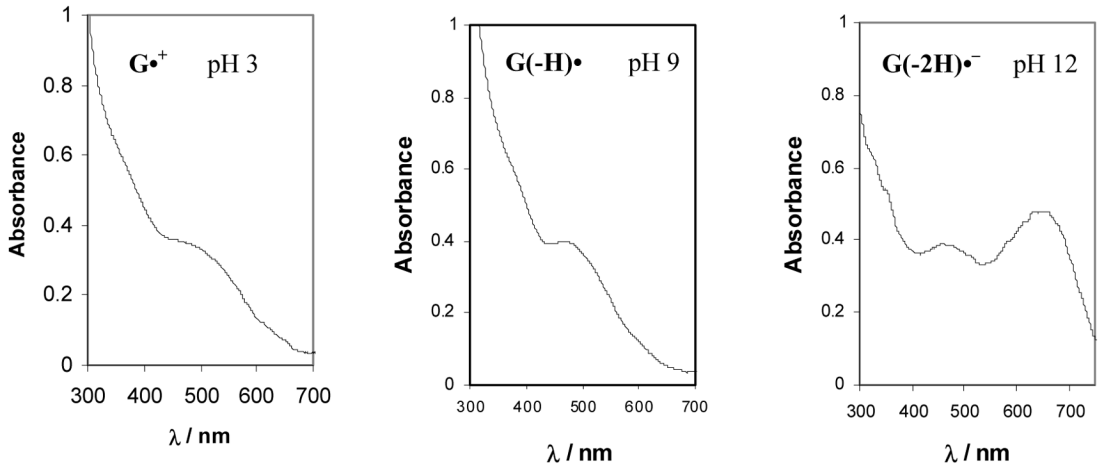

Figure 1.

The uv-visible absorption spectra of one-electron oxidized guanine moiety- $G^{\bullet+}$, G(-H)• and $G(-2H)^{\bullet-}$ respectively produced by $Cl_2^{\bullet-}$ oxidation of dGuo, at 77 K in 7.5 *M* LiCl glass/D_2O with pH.

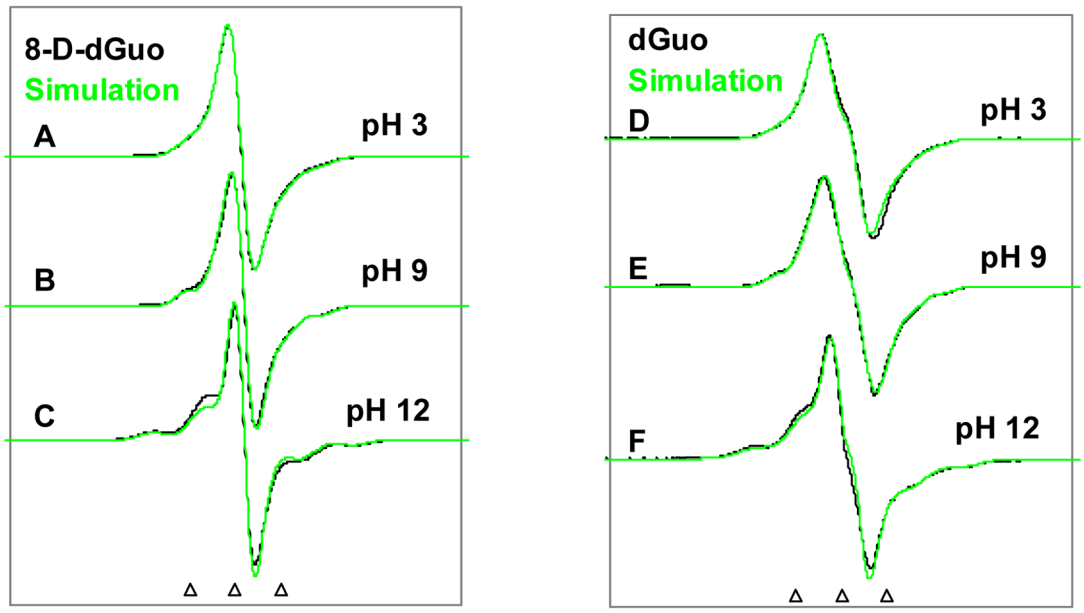

Figure 2.

ESR spectra found for one-electron oxidized 8-D-dGuo (A – C) (black), dGuo (D – F) (black) at various pHs in 7.5 *M* LiCl glasses at 77 K. The ESR parameters, hyperfine couplings and g-values, used for the simulated spectra (green) are given in Table 1. Our results indicate that G•$^{+}$ is found at pHs ≤5, G(N1-H)• is found at pH 7–9 and G(-2H)•$^{-}$ is found at pH ca.12. All spectra were recorded at 77 K. The three reference markers in all figures are Fremy's salt resonances with central marker is at g= 2.0056, and each of three markers is separated from one another by 13.09 G.

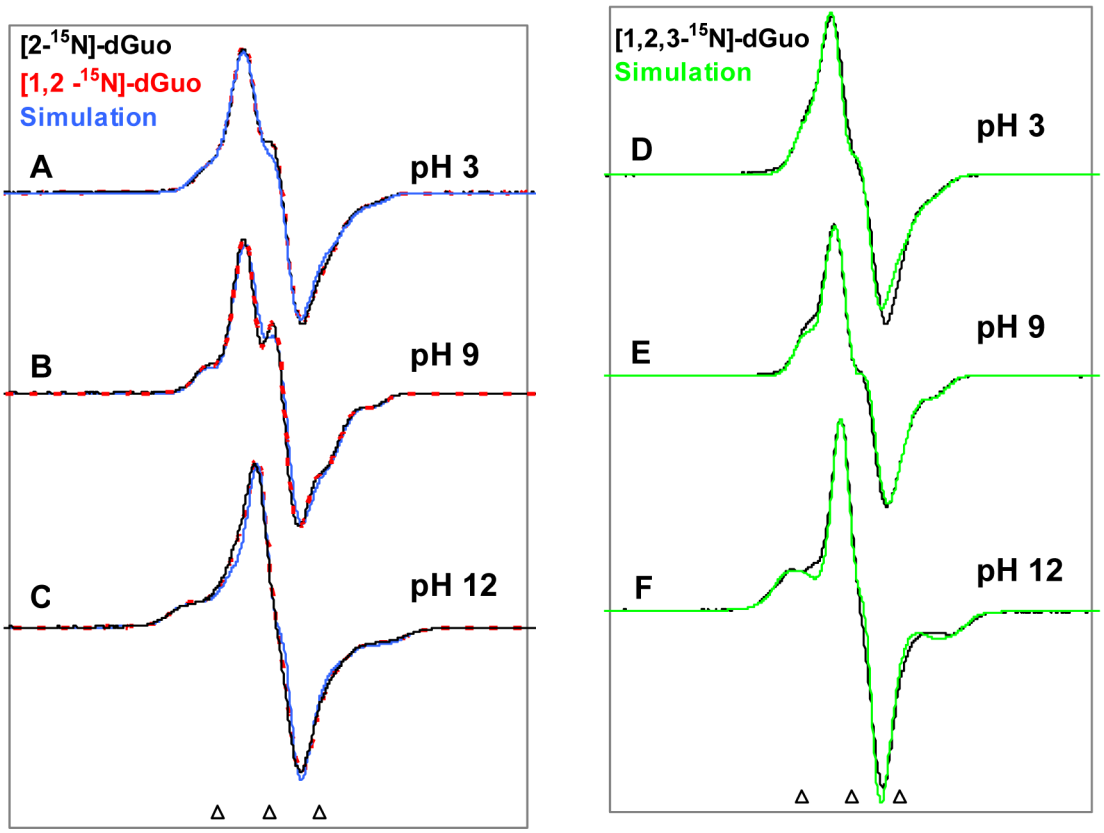

Figure 3.

ESR spectra found for one-electron oxidized [2-^{15}N]-dGuo (Black) and [1,2-^{15}N]-dGuo (broken red) (A - C), [1,2,3-^{15}N]-dGuo (black) (D – F) at various pHs in 7.5 *M* LiCl glasses at 77 K. The ESR parameters, hyperfine couplings and g-values, used for the simulated spectra are given in Tables 1 with ^{15}N (spin =1/2) couplings at ^{15}N-substituted sites equal to 1.404 times the ^{14}N (spin =1) couplings. The close fits of the simulated spectra in black and the experiment both verify the ^{14}N coupling magnitudes as well as the sites of the couplings. In A-C the fact that [2-^{15}N]-dGuo and [1,2-^{15}N]-dGuo give identical spectra shows that the N1 site does not have a significant coupling.

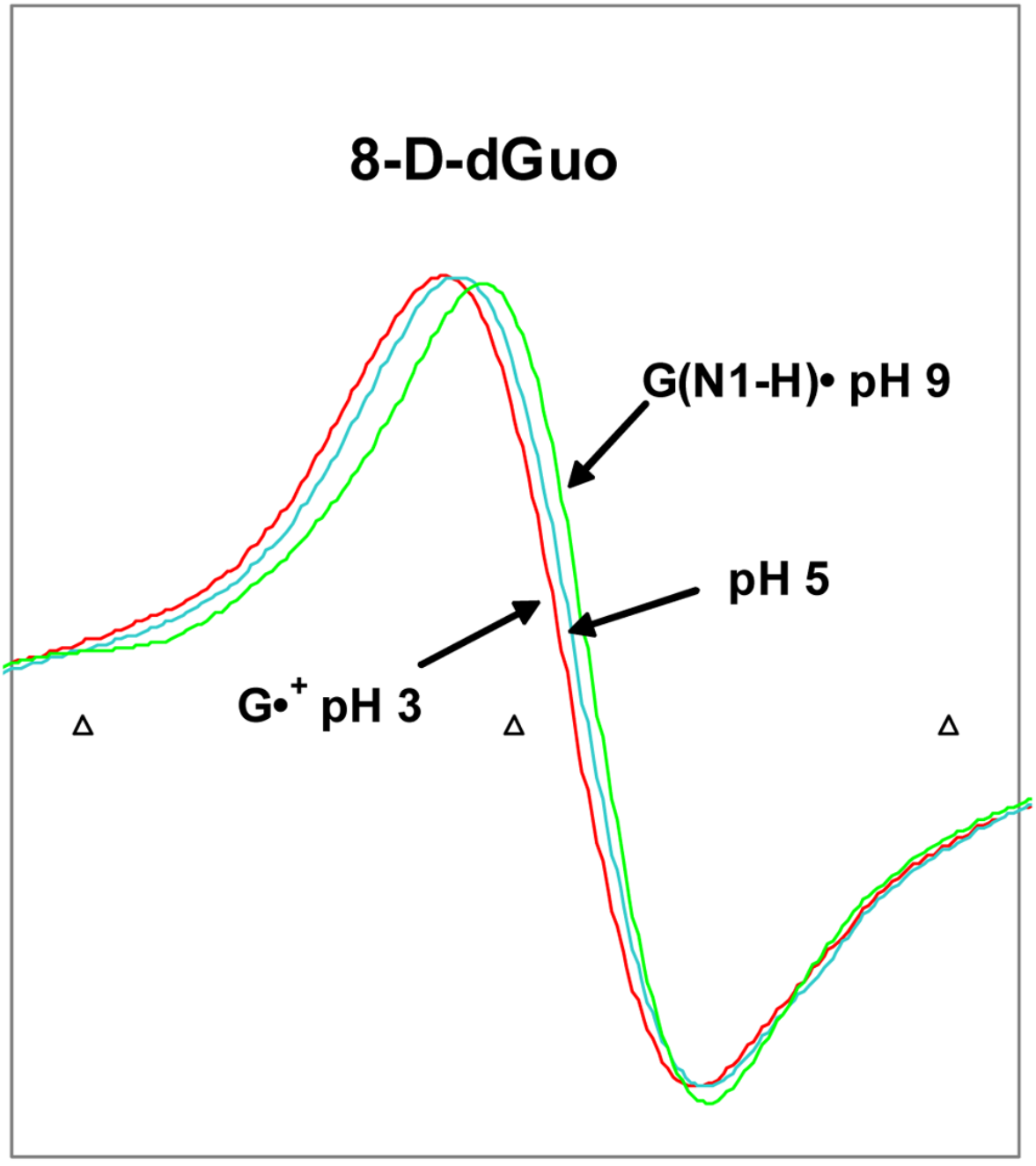

Figure 4.
ESR spectra for one-electron oxidized 8-D-dGuo in a 7.5 *M* LiCl glass at 77 K showing the difference in the field positions of the central components (apparent g⊥ values) of G•$^{+}$ (pH=3) and G(N1-H)• (pH=9). The fact that the apparent g-value of the ESR spectrum at pH 5 is near the average of those obtained at pH 3 and pH 9 suggests that, at pH = 5, about equal amounts of G(N1-H)• and G•$^{+}$ are present.

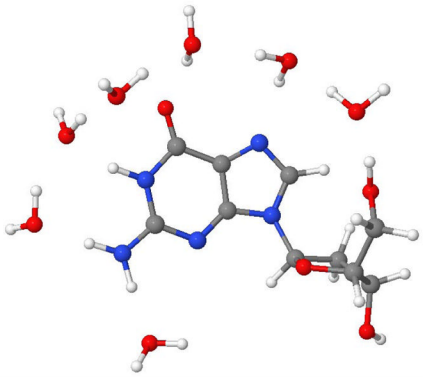

(a) $G^{\bullet+} + 7H_2O$

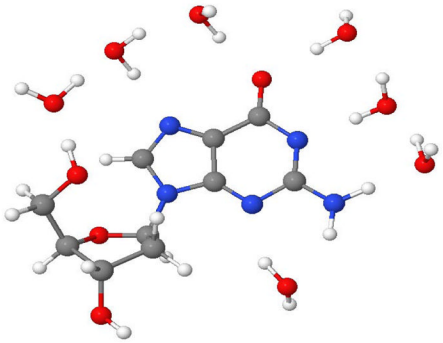

(b) $G(N1\text{-}H)^{\bullet} + 7H_2O$

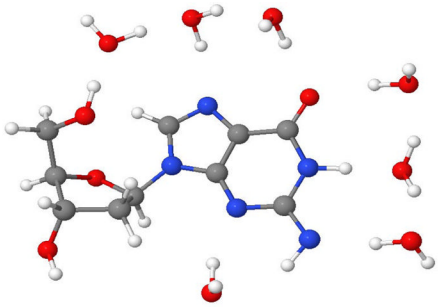

(c) $G(N2\text{-}H)^{\bullet}_{syn} + 7H_2O$

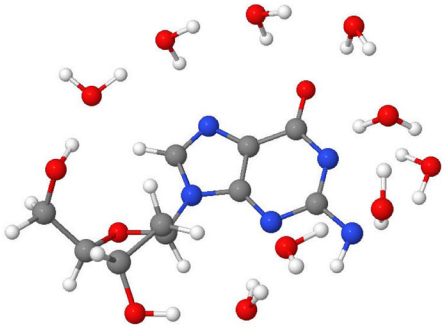

(d) $G(-2H)^{\bullet-} + 9H_2O$

Figure 5.

Optimized structures of (a) $G^{\bullet+}$, (b) $G(N1\text{-}H)^{\bullet}$, (c) $G(N2\text{-}H)^{\bullet}_{syn}$ and (d) $G(-2H)^{\bullet-}$ in the presence of water molecules. The geometries were fully optimized using B3LYP/6-31G(d) method.

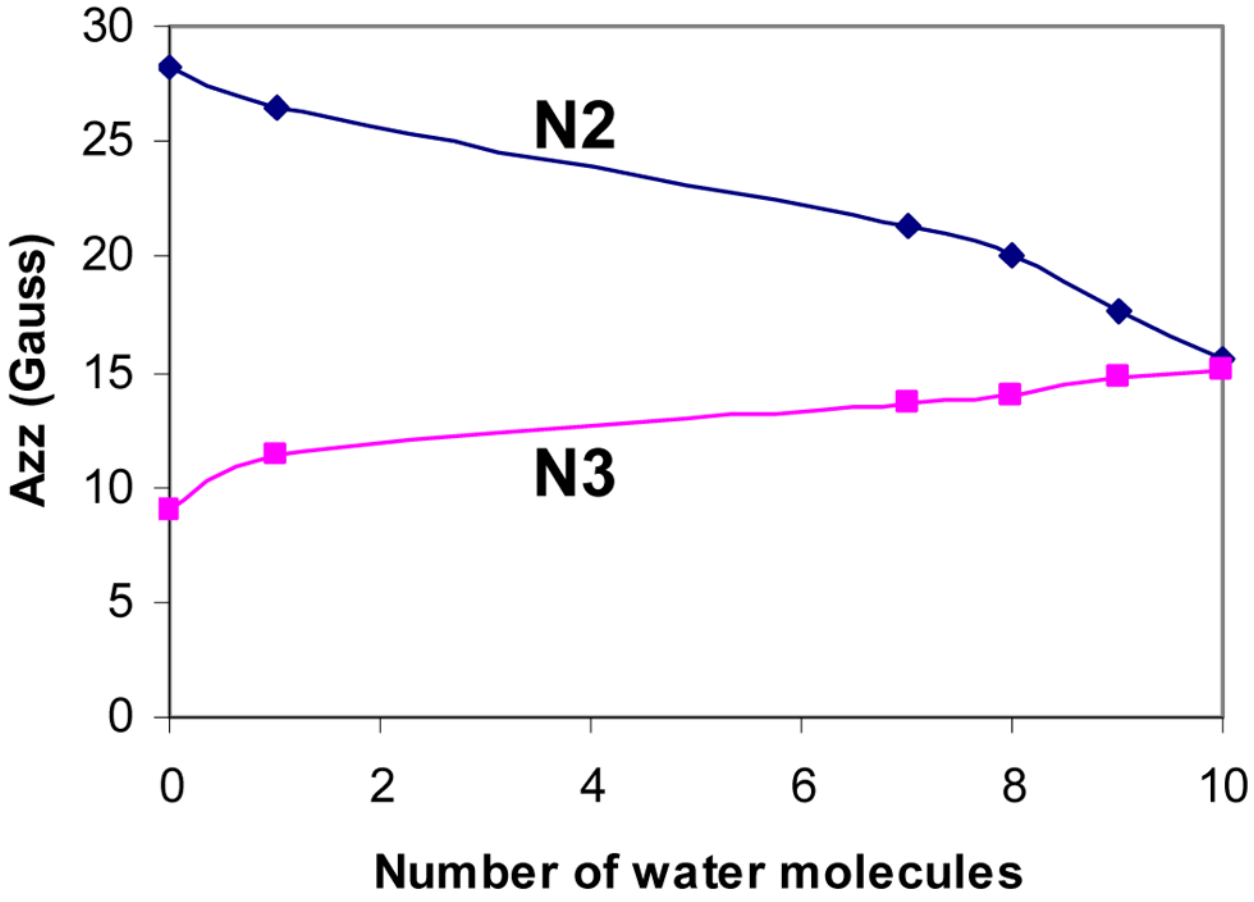

Figure 6.
Variation of hyperfine coupling constant A_{zz} (Gauss) at N2 and at N3 sites of G(-2H)•⁻ with number of water molecules of hydration. Calculations were done using B3LYP/6-31G(d) method.

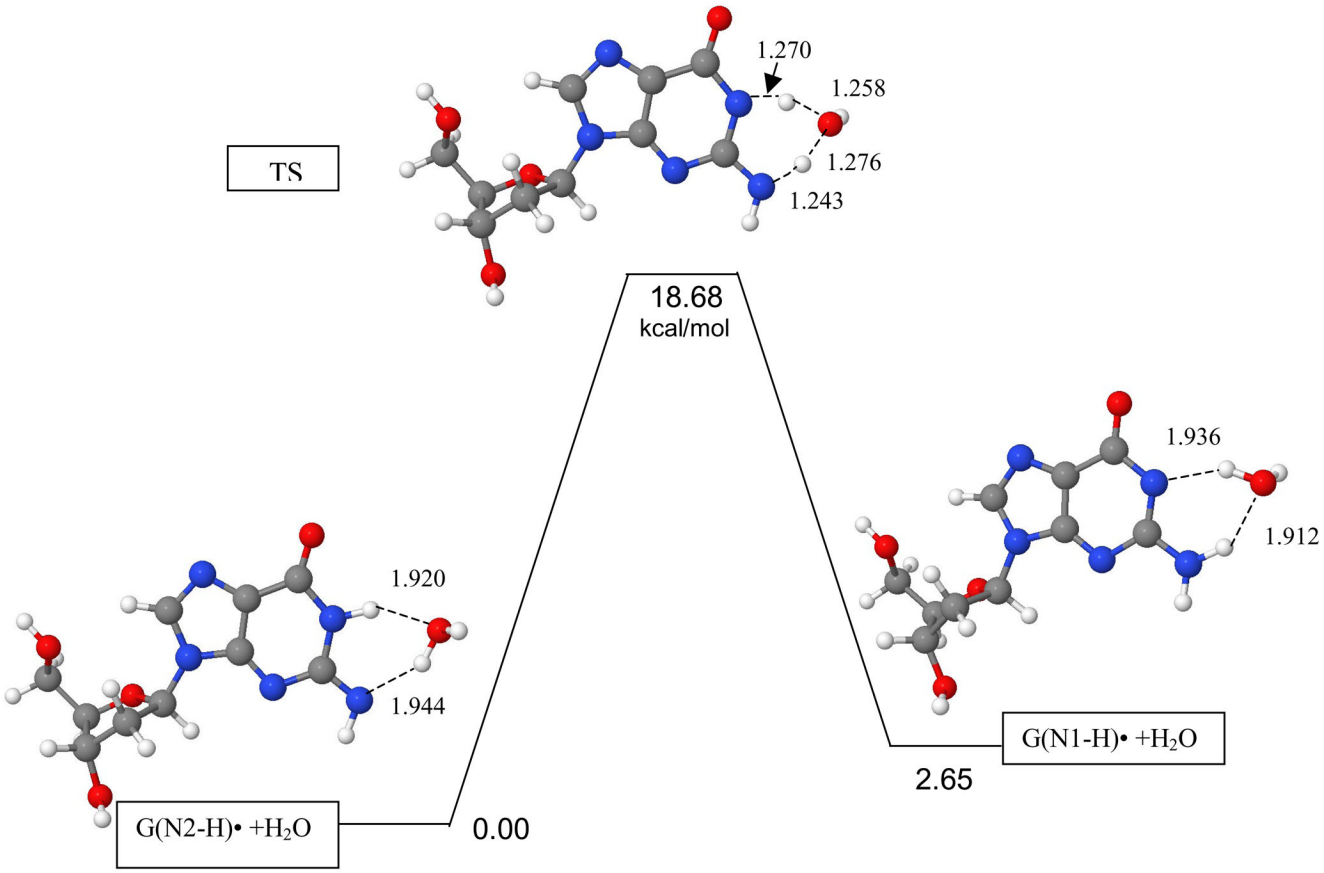

Figure 7.
Water assisted proton transfer reaction path between G(N2-H)•$_{syn}$+H_2O and G(N1-H)•+H_2O through the transition state.The geometries were optimized and energies calculated using the B3LYP/6-31G(d) level of calculation. Bond distances in Å and energies in kcal/mol.

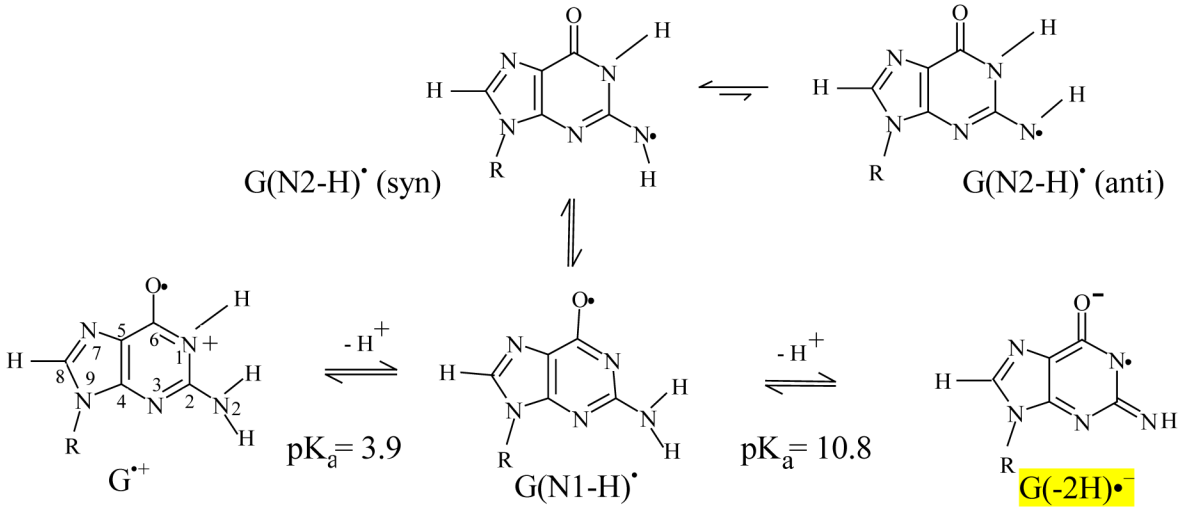

Scheme 1.

Prototropic equilibria of one-electron oxidized guanine including the cation radical ($G^{\bullet+}$), the mono- deprotonated species, (G(N1-H)• and G(N2-H)•, in syn and anti- conformers with respect to the N3 atom) and the di- deprotonated species, $G(-2H)^{\bullet-}$). The numbering scheme in shown here is followed in this work.

Table 1

Experimental and Theoretical[a] ESR Parameters for G•$^{+}$, G(-H)• and G(-2H)•$^{-}$

Radical		8-D-dGuo/dGuo[b]						dGuo			8-D-dGuo/dGuo
		^{14}N3 couplings(G)			^{14}N2 couplings(G)			C8(H) Coupling (G)			g-values (experimental)
		A_{zz}	A_{xx}	A_{yy}	A_{zz}	A_{xx}	A_{yy}	A_{zz}	A_{xx}	A_{yy}	
G•$^{+}$	**Exp** [c,d,e]	13.0	~0	~0	6.5	~0	~0	−7.5	−10.5	−3.5	g_{xx}=2.0045
	Theory										g_{yy}=2.0045
	+ 7 H_2O	11.8	0.8	0.8	9.1	0.6	0.6	−7.8	−10.4	−2.4	g_{zz}=2.0021
G(-H)•	**Exp** [c,d,e]	12.0	~0	~0	8.0	~0	~0	−7.2	−10.5	−3.5	g_{xx}=2.0041
	Theory										g_{yy}=2.0041
	G(N1-H)• + 7 H_2O	13.5	0.8	0.9	9.1	0.6	0.7	−8.4	−11.3	−3.0	g_{zz}=2.0021
	G(N2-H)• + 7 H_2O	15.0	1.0	1.0	17.6	0.8	0.8	−6.6	−8.8	−2.3	
G(-2H)•$^{-}$	**Exp** [c,d,e]	13.2	~0	~0	16.2	~0	~0	−5.5	−7.5	−2.5	g_{xx}=2.0042
	Theory										g_{yy}=2.0042
	+9 H_2O	14.8	0.9	1.0	17.6	0.8	0.8	−6.8	−9.3	−2.6	g_{zz}=2.0025
	+10 H_2O	15.1	1.0	1.0	15.5	0.7	0.7	−7.2	−9.8	−2.7	

[a] Structures optimized and hyperfine couplings calculated using DFT (B3LYP) with a 6-31G(d) basis set.

[b] Experimental nitrogen hyperfine couplings and g values were measured in 8-D-dGuo and these were then employed to simulate the spectra of G•$^{+}$, G(-H)• and G(-2H)•$^{-}$ in dGuo.

[c] Experimental A_{XX} and A_{yy} nitrogen hyperfine couplings of value ca. zero are within the line-width and too small to be characterized. Theoretical values confirm the small values of these couplings.

[d] Line-shapes used were generally Lorenztian for the 8-D-dGuo and Gaussian for dGuo radical species. The C8(H) coupling creates a superposition of line components at various orientations best simulated with the Gaussian lineshape.

[e] ^{15}N (spin=1/2) couplings are 1.404 times the nitrogen couplings (^{14}N, spin=1) shown above.

Table 2

Relative stabilities of G(N1-H)• and G(N2-H)• calculated using different methods and basis sets.

Method	Ref	Parent Structure	Relative stability (kcal/mol)	
			G(N1-H)•	G(N2-H)•[a]
B3LYP/6-31G	This work	dGuo+H_2O (solution)[b]	2.65 (0.90)	0.00, 3.63 *anti* (0.00)
B3LYP/6-31G	This work	dGuo+7 H_2O (solution)[b]	0.00 (0.00)	3.26 (3.00)
B3LYP/6-31G*[c]	This Work	9-Met-Gua H_2O	2.80	0.00
B3LYP/6-31++G(3df,3pd)//B3LYP/6-31++G(3df,3pd)[d]	6b	Guanine (solution)	4.71 (0.00)	0.00 (0.91)
B3LYP/6-311G(2pd,p)//6-31G**	6b	Guanine	4.43[e]	0.00
CPMD[f]	6b	Guanine	3.73	0.00
B3LYP/DZP++[g]	6d	Guanine	4.96	0.00, 4.76 *anti*

[a] Unless and otherwise stated G(N2-H)• refers to syn conformer, G(N2-H)•syn.

[b] PCM solvation model.

[c] Relative stabilities calculated by us by substituting methyl (CH_3) group at the N9 site of the guanine radical in the presence of a single water molecule placed between N1 and N2 side of the 9-methyl guanine radical.

[d] The solvation free energies using COSMO model are given in the parentheses.

[e] Enthalpy calculated at 0 K.

[f] Car-Parrinello molecular dynamics (CPMD) method

[g] Zero-point vibration corrected energies.

Table 3

B3LYP/6-31G(d) calculated hyperfine coupling constants (HFCCs) and spin densities at different atoms of G•$^{+}$, G(N1-H)•, G(N2-H)• and G(-2H)•$^{-}$ in presence of seven water molecules as shown in scheme 1.

Species	Atom No.	Spin densities	Hyperfine couplings (Gauss)[a]			
			a_{iso}	T_{zz}	T_{yy}	T_{xx}
G•$^{+}$+7H_2O	N1	−0.019	−0.70	0.38	0.32	−0.65
	N2	0.190	3.41	5.67	−2.79	−2.88
	N3	0.245	4.33	7.51	−3.48	−3.54
	N7	0.025	0.51	1.46	−0.70	−0.77
	C8---H	0.226[b]	−6.86	−0.91	4.41	−3.50
G(N1-H)• + 7H_2O	N1	−0.018	−0.47	0.30	0.28	−0.58
	N2	0.188	3.44	5.63	−2.77	−2.87
	N3	0.281	5.08	8.44	−4.21	−4.23
	N7	−0.009	−0.06	0.56	−0.24	−0.32
	C8---H	0.245[b]	−7.58	−0.81	4.55	−3.74
G(N2-H)• + 7H_2O	N1	0.027	0.34	1.78	−0.85	−0.33
	N2	0.399	6.47	11.16	−5.57	−5.60
	N3	0.316	5.69	9.34	−4.63	−4.71
	N7	−0.003	0.00	0.63	−0.29	−0.34
	C8---H	0.189[b]	−5.90	−0.66	3.59	−2.93
G(-2H)•$^{-}$ + 9H_2O	N1	0.030	0.34	0.75	−0.35	−0.40
	N2	0.397	6.4	11.24	−5.61	−5.63
	N3	0.314	5.59	9.23	−4.57	−4.66
	N7	−0.038	−0.56	0.23	0.16	−0.39
	C8---H	0.202[b]	−6.23	−0.56	3.63	−3.06
G(-2H)•$^{-}$ + 10H_2O	N1	0.016	0.07	0.34	−0.14	−0.20
	N2	0.347	5.65	9.82	−4.91	−4.91
	N3	0.320	5.71	9.41	−4.67	−4.75
	N7	−0.036	−0.52	0.22	0.12	−0.34
	C8---H	0.213[b]	−6.56	−0.60	3.82	−3.22

[a] $A_{ii} = a_{iso} + T_{ii}$, as discussed in the text.

[b] The spin density on the C atom at C-8.